

Nanofriction behavior of cluster-assembled carbon films

A. Podestà, G. Fantoni, P. Milani*

*INFN - Dipartimento di Fisica, Università di Milano,
Via Celoria 16, 20133 Milano, Italy*

M. Ragazzi, D. Donadio

*INFN - Dipartimento di Scienza dei Materiali,
Università di Milano-Bicocca,
Via Cozzi 53, 20125 Milano, Italy*

L. Colombo

*INFN - Dipartimento di Fisica, Università di Cagliari,
Cittadella Universitaria 09042 Monserrato (CA), Italy*

(Dated: February 6, 2008)

Abstract

We have characterized the frictional properties of nanostructured (ns) carbon films grown by Supersonic Cluster Beam Deposition (SCBD) via an Atomic Force-Friction Force Microscope (AFM-FFM). The experimental data are discussed on the basis of a modified Amonton's law for friction, stating a linear dependence of friction on load plus an adhesive offset accounting for a finite friction force in the limit of null total applied load. Molecular Dynamics simulations of the interaction of the AFM tip with the nanostructured carbon confirm the validity of the friction model used for this system. Experimental results show that the friction coefficient is not influenced by the nanostructure of the films nor by the relative humidity. On the other hand the adhesion coefficient depends on these parameters.

Keywords: Nanotribology; AFM; friction; carbon; cluster-assembled materials

1. INTRODUCTION

The understanding and control of friction, adhesion, lubrication and wear in nanostructured systems is an essential requisite to validate the use of nanomaterials for highly demanding structural applications^{1,2}. The rapidly growing number of applications based on microelectromechanical systems (MEMS) and the new perspectives opened by the production of nano electromechanical systems (NEMS) make necessary the development of an entirely novel class of protective and lubricant coatings with improved mechanical properties at the nanoscale³. Carbon-based materials have emerged as a promising class of materials⁴. Diamond and the various types of amorphous carbon show interesting tribological properties such as high elastic moduli, good lubrication properties, low stiction surfaces, etc.⁴. These properties are controlled by a combination of physico-chemical properties of the surfaces such as sp²/sp³ ratio, surface roughness and porosity and by the presence of contaminant layers⁵.

Cluster-assembled carbon represents a novel nanostructured material obtained by the deposition of clusters produced in a supersonic expansion⁶. Cluster-assembled carbon films can be obtained starting from cluster mass distributions that contain clusters with fullerene-like structure and/or linear and planar structures⁷. Low-energy deposition (fractions of eV per atom) drastically reduces fragmentation on the substrate allowing the films to be structured at the nano- and mesoscale by keeping memory of the original cluster distribution⁸. The mechanical properties of cluster-assembled carbon films have been studied by Brillouin light scattering showing that these systems have elastic properties similar to graphite (shear modulus) and Young modulus and Poisson's ratio typical of a soft very porous material (note that the Poisson's ratio is very close to zero or, in certain cases, even negative)⁹.

The Atomic Force-Friction Force Microscope (AFM-FFM) has emerged as a powerful tool for the characterization of the tribological properties of materials from the micrometer down to the atomic scale^{2,10}. However, the use of a nanometer-sized probe in nano-friction experiments carried out on corrugated samples in humid environments causes the experimental conditions to be usually different from both those encountered in typical ultra high-vacuum experiments, where flat crystalline surfaces are investigated in a humidity and contaminants-free environment, leading to a single-asperity contact, and those of macroscopic tribology, where the contact regime is always multi-asperity like¹¹. A number of parameters such as

adhesion, surface and tip micro and nano-roughness, load range, as well as tip radius and shape, influence the contact-friction regime. Moreover, local corrugation on a scale larger than that of the probe can affect the friction measurement^{12,13}. The case of nanostructured materials is somehow peculiar since the typical size of the probe is close to or even comparable with cluster size. In this case peculiar tip-sample interactions and topographic effects should be expected.

In this paper we present the results of an AFM-FFM characterization of the frictional properties of cluster-assembled carbon films. We have studied the dependence of frictional parameters on both the relative humidity and the structural composition of films deposited with different cluster mass distributions.

The experimental data are discussed on the basis of a modified Amonton's law for friction¹⁴, stating a linear dependence of friction on load plus an adhesive offset accounting for a finite friction force in the limit of null total applied load. A new procedure for the correction of the lateral force maps from the contributions of the local tilt of the surface (the topographic correction) was applied in order to extract intrinsic values of the frictional parameters independent on surface roughness on a scale larger than that of the tip-sample contact. In order to validate the use of the Amonton's law for the interpretation of the experimental data, we have simulated the AFM tip-nanostructured carbon interaction via molecular dynamics (MD) simulations. MD results of the nanofriction experiment support the validity of the friction model used for this system.

2. EXPERIMENTAL DETAILS

2.1. Deposition of nanostructured carbon

The use of supersonic beams of clusters for deposition of thin films has attracted a large interest from more than two decades¹⁵. This technique consists in preparing clusters in the gas phase diluted in a carrier light inert gas, typically Helium, and letting the mixture expand through a nozzle in high vacuum so that a very collimated, intense supersonic beam is produced. The cluster beam is intercepted by a suitable substrate in order to deposit a thin film. In the case of carbon, the kinetic energy per atom in the clusters (below 0.4 eV/atom) is smaller than the binding energy per atom avoiding massive fragmentation: the

resulting film has a structure at the nanoscale keeping the memory of the nanometer-sized building blocks used for the assembling.

Nanostructured carbon films have been deposited from a supersonic cluster beam produced by a pulsed microplasma cluster source (PMCS) as described in detail in Ref. 16. With normal PMCS operation conditions, the cluster beam is characterized by a log-normal cluster mass distribution peaked at about 500 atoms/cluster and extending to several thousands atoms per cluster. We have controlled and varied the cluster mass distribution and deposition rates by exploiting aerodynamic focusing effects¹⁷. Using the standard cluster mass distribution described above, we have deposited films with thicknesses of several hundreds of nanometers on silicon substrates. The deposition rate was 4-5 nm/min and the density of the films was 0.8-0.9 g/cm³. With a suitable nozzle configuration we have produced a beam depleted from clusters with diameters roughly larger than 2 nm¹⁷. These conditions produce films with densities of 1.2-1.3 g/cm³ at a deposition rate of 5 nm/sec.

Raman analysis have shown that in films grown with large clusters the graphitic *sp*² bonding, due to the large number of cage-like particles, is more pronounced than in films grown with small clusters, whose structure resembles more that of the amorphous carbon. In the following, we shall refer to films grown with the two different nozzles as to the films grown with small and large clusters, accordingly.

2.2. AFM-FFM

The atomic force microscope is a Nanoscope Multimode IIIa from Digital Instruments with phase extender and Signal Acquisition Module (SAM). We scanned different points of the samples, with scan size 500 nm, sliding velocity typically 1 μ m/s. We used rectangular cantilevers 450 μ m long with silicon tip with radius 5-40 nm. The AFM can be housed in a sealed chamber connected to a humidifier to work in controlled humidity and atmosphere (typically in dry and wet nitrogen). A second PC is used to remotely control the external applied load in friction measurements. The application of the external load is synchronized via the reading of the end-line and end-frame triggers from the microscope. We can acquire a complete friction vs. load curve in a single AFM scan of typically 512 lines, 512 points per line. This allows performing many measurements in each session, fast and reliably. The experimental data are extracted in ASCII format and processed via dedicated software.

3. MOLECULAR DYNAMICS SIMULATIONS

The theoretical investigation has been carried out by classical MD simulations based on the Tersoff potential¹⁸. This computational framework has proved to be reliable for the investigation of the structural properties of carbon based materials¹⁹ and particularly of nanostructured cluster assembled carbon films. The growth of nanostructured carbon films by supersonic cluster beam deposition on a (001) diamond substrate has been simulated by a protocol described in Ref. 7 which accounts well for the experimental deposition process. The simulation cell is a slab with periodic boundary conditions applied in the plane orthogonal to the growth direction, the substrate is four layers thick and its bottom layer is rigid, while the second and third layers are thermostat. The dynamics of the atoms of the forth layer is newtonian as that of the impinging clusters. Two samples have been produced with the same growth conditions (cluster kinetic energy, vibrational temperature, substrate temperature) but different size distribution of the precursors: sample (A) has been obtained from a cluster beam mostly containing small precursors (1 to 23 atoms per cluster) and sample (B) has been grown mainly from larger precursors (46 to 120 atoms per cluster). The structural properties of the two sample, which are strongly influenced by the features of the precursors, are discussed elsewhere⁷.

Fig. 1 illustrates the molecular dynamics model for the FFM experiment: a small crystalline diamond tip slides on the surface of the nanostructured carbon. The tip consists of 178 carbon atoms arranged in a truncated pyramid shape, obtained by cutting an ideal diamond structure crystal along (111) and (001) directions and letting it relax at room temperature. Tip radius is about 8 Å. Although silicon tips are used in experimental measurements we have chosen to perform nanofriction simulations with a stiffer carbon tip, in order to avoid the complete wearing of the tip even at relatively low normal loads, due to its small size. Thus it has been possible to perform FFM simulations with loads up to 30 nN. Since the thickness of the samples exploited for nano-friction simulations is about 60 Å, in order to reduce computational costs, a 20 Å thick layer of the film is fixed, the atoms belonging to the 2 Å thick layer above it are thermostat and the dynamics of the other atoms of the film is Newtonian. The two top layers of the tip are rigid and they are subject to the external forces that mimic the action of the AFM cantilever. The overall external force acting on the tip has been decomposed into three independent components: (i) an elastic

dragging force that produces the sliding motion of the tip, (ii) a constant load perpendicular to the sliding plane and (iii) an elastic torsion force that keeps the tip vertical with respect to the sliding plane. The frictional force is calculated at every timestep as the reaction to the elastic dragging force and it is averaged over six paths 20 Å long.

Since the formation of chemical bonds between the atoms of the AFM tip and those of the film is quite unlikely in such AFM-FFM experiments, the film–tip interaction is ruled by Van der Waals forces. Therefore the film–tip interaction is modelled by a two-body modified Morse potential given by:

$$V(r_{ij}) = D(e^{-2\alpha(r_{ij}-d-r_0)} - 2e^{\alpha(r_{ij}-r_0)}), \quad (1)$$

where r_{ij} is the distance between two atoms. As for D and α parameters we have chosen the values fitted by Cheong et al.²⁰: namely $D = 0.435$ eV and $\alpha = 46.487$. The parameter d has been introduced in order to increase the equilibrium distance and to reduce the binding energy between the tip and the film. This reproduces better the actual experimental conditions: as the FFM measurements are usually performed in air, we have to assume that the surface-tip interaction is modified by hydrogen passivation of the dangling bonds and by the presence of surface lubricants or contaminants. Hence, in principle, by tuning this parameter one may study the effects of lubricants and contaminants without explicitly introduce them. We have chosen $d = 0.011$ nm, by performing sliding friction simulations on the (001) non reconstructed surface of diamond and comparing the calculated lateral force to those measured in Ref. 21.

4. RESULTS AND DISCUSSION

4.1. AFM-FFM measurements

Our characterization protocol assumes a modified Amonton’s law for friction, i.e. a linear dependence on total load plus an offset representing the zero-load friction force in analogy with the single-asperity JKR contact model²²:

$$f = \mu N + c \quad (2)$$

Here N represents the *total* applied load in the direction perpendicular to the surface, including the contribution of adhesion A , and c accounts for a zero-load friction force.

We apply a procedure, described in details elsewhere^{23,24}, to correct lateral force maps from the spurious contributions due to the presence of a local tilt of the surface. Actually, in the case of a locally tilted surface, the measured forces in the directions parallel and perpendicular to the AFM reference plane do not necessarily coincide with the forces acting parallel and perpendicularly to the sample surface, which actually define the friction coefficient and the friction vs. load characteristics of the interface under investigation. The topographic correction is necessary in order to extract quantitative and accurate information from corrugated sample and to compare results from different samples.

We have investigated frictional properties of films grown with large and small clusters in dry and humid nitrogen environment. In Fig. 2 are shown two AFM pictures at different magnifications of a 250 nm thick ns-carbon film. Typical film morphology consists in a fine raster of grains with typical diameter of 10-20 nm. Films grown with large clusters are usually rougher than films grown with small clusters with the same thickness. However, our protocol automatically corrects the friction maps for the topographic contributions, allowing the comparison of the results obtained on different samples.

In Fig. 3 is shown a typical lateral force vs. applied load curve measured on ns-carbon. This curve is obtained extracting from the original lateral force-load dispersion the subset of all the lateral force-load pairs corresponding to the same slope in the topographic map. Each of such curves is processed separately in order to apply the topographic correction.

We show in Fig. 4 the measured *dynamic* friction coefficients and friction offsets for the film grown with large clusters and grown with small clusters accordingly, measured in ambient condition (RH \sim 40%)³⁵. The average values for both μ and c are:

$$\begin{aligned}\mu_{large}^{humid} &= 0.086 \pm 0.013, & c_{large}^{humid} &= 0.44 \pm 0.29 \text{ nN} \\ \mu_{small}^{humid} &= 0.085 \pm 0.007, & c_{small}^{humid} &= 0.26 \pm 0.15 \text{ nN}\end{aligned}\tag{3}$$

We also studied the frictional behavior of ns-carbon film in dry environment (RH \sim 2%). The results are shown in Fig. 5. The averaged values are:

$$\begin{aligned}\mu_{large}^{dry} &= 0.081 \pm 0.012, & c_{large}^{dry} &= 0.69 \pm 0.28 \text{ nN} \\ \mu_{small}^{dry} &= 0.082 \pm 0.008, & c_{small}^{dry} &= 0.47 \pm 0.20 \text{ nN}\end{aligned}\tag{4}$$

The errors shown in Eqs. 3 and 4 are calculated as: $\sigma = 1/N \sqrt{\sum \sigma_i^2}$, where σ_i are the errors associated to each measurements.

4.2. MD results

Exploiting the model setup described in Section 3, we have performed several nanofriction simulations, calculating the values of lateral friction force as a function of the applied normal load, both for sample (A) and for sample (B). Each simulated measurement at a fixed load, consists of six independent scannings 25 Å long. The friction force for each scansion is obtained by the average of the lateral force calculated at every time-step of the simulation and the values reported in Fig. 6 are calculated by averaging over the six scannings. This procedure provides a sufficient amount of data so to devise a linear trend in the lateral force as a function of applied load and to calculate the slope, i.e. the friction coefficient, and the offset of the curves according to the modified Amonton's law discussed above. The friction coefficient and offset values thus obtained are:

$$\begin{aligned}\mu^A &= 0.47 \pm 0.110, & c^A &= 1.81 \pm 1.43, nN \\ \mu^B &= 0.42 \pm 0.053, & c^B &= 0.70 \pm 0.59, nN\end{aligned}\tag{5}$$

Simulation have been performed with loads up to 22.6 nN for sample (A) and 19.2 nN for sample (B). Beyond these threshold values, combined wearing of the tip and of the film occurs and lateral force rapidly increases above the linear behavior observed so far.

No topographic correction to the theoretically calculated friction vs. load curves has been applied, since the method used to calculate each single point of the curves averages over the scanned profile and this should already account for the topographic effects. Moreover, the average tilt angle of the MD profiles is in general smaller than 15 degrees, making the topographic correction negligible.

4.3. Discussion

The observed lateral force vs. applied load curves for ns-carbon are linear, except for very low loads, close to the pull-off limit, and for loads larger than about 30 nN (Fig. 3). Moreover, in the limit of the experimental error, the measured values of the friction offset are definitely different from zero. These observations confirm that the friction law of a silicon tip on cluster-assembled carbon is well represented by an Amonton's like equation, and in addition that a zero-load offset must be included in the friction model.

MD results further support our model based on a modified Amonton's law. Simulations show a linear trend of the friction vs. load curve with a finite offset, different from zero in the limit of the experimental error. The quantitative discrepancy between theoretical and experimental results is not surprising and it can be attributed to the parameterization of the interaction potentials and in the choice of using carbon tips in the simulations of the FFM experiments.

For loads larger than about 30 nN we have evidence of the onset of non-linear trends in friction vs. load curves, probably related to wear and indentation during scanning. The phenomenon of wearing of the ns-carbon film has been directly observed in MD simulations at loads larger than 30 nN.

It has been reported that the values of the friction coefficients measured in successive scans are likely to be different^{2,25}. This is currently attributed to modification of the tip-sample interface after repeated sliding due to material removal, tip wear and blunting and even structural modifications. Blunting of the tip is a very unlikely event in this case because Silicon is much harder than cluster-assembled carbon. The observed fluctuations in the measured parameters (see Figs. 4 and 5) could be attributed to dynamic modifications of the contact area during sliding because of the contamination of the AFM tip, which may pick up carbon during scanning, particularly at higher loads, and even indent the film, which is much softer than the tip.

The strongest fluctuations are observed for the experimental friction offset c . This is not surprising, because this parameter is expected to be highly dependent not only upon environmental conditions (such as relative humidity and temperature), but also upon tip shape and contamination, these being the parameters directly influencing adhesion. This fact is clearly represented by the large errors in the measured adhesive offset. While the relative error for the friction coefficient are below 15%, which is basically the limit set by the accuracy of the calibration procedure for the force constants of the cantilever^{26,36}, those of the adhesive offset are as large as 60%. In the absence of an accurate characterization of tip shape and size however it is not possible to definitely individuate the causes of the observed changes in the friction offset c . The investigation of adhesive properties of cluster-assembled carbon should be more reliable through the analysis of force vs. distance curves, or even via the study of thermal fluctuations of the cantilever close to the nanostructured surface, provided a reliable model of the tip-sample interaction and/or contact.

As confirmed also by MD simulations, in the limit of the experimental error, the nanostructure of the films seems to have very weak or no influence on the friction coefficient. In analogy to the macroscale, one could expect that films grown with large clusters and hence containing a larger number of well-organized graphitic regions should show a lower friction coefficient²⁷. This is not observed.

The friction coefficient is also found to be independent on relative humidity. Null or weak dependence of friction coefficient and adhesion on the relative humidity was reported in literature for carbon-based materials^{25,28,29}. One possible explanation for the behavior of our films in dry environment is the hydrophilic nature of cluster-assembled carbon³⁰. The low density and large porosity of these systems in conjunction with a non-negligible wettability may favor the formation of a water layer lasting even in dry nitrogen with the formation of a water meniscus between the tip and the surface

Friction coefficients measured on carbon-based materials span from 0.009 (for HOPG in air) to 1 for DLC in UHV²⁷. A numerical comparison with nanostructured carbon would not be of great interest because of the large scattering of the results and the arbitrariness of the calibration procedures adopted. What is in general observed is that all carbon-based materials are better lubricants in the presence of surface contamination, while in very clean and dry environments the covalent interaction between sample and probe (usually Silicon or Diamond) leads to higher friction coefficients. In the case of cluster-assembled carbon we do not observe an increase of the friction coefficient upon removal of the environmental humidity.

The adhesive offset c is found experimentally to decrease in humid environment. The decrease of the adhesion force with increasing relative humidity was observed in other systems²⁸. This is explained by a decrease of the capillary attractive force exerted by the water meniscus in the tip-surface gap, with higher relative humidity, upon a certain threshold, depending on the material. This could explain also the larger adhesion coefficient observed in the films grown from large clusters. This system with a more pronounced graphitic character may have a smaller wettability compared to that grown by small clusters³⁰.

In the simulations the effect of humidity is poorly reproduced by the introduction of the parameter d in the empirical potential describing the tip-film interaction since it is impossible to establish a clear relation between the relative humidity and the value of d . Anyway, we have observed that in completely dry conditions, corresponding to $d = 0$ Å, strong adhesion

of the tip on the surface occurs, resulting in the complete wearing of the tip and in large deformation of the scanned surface, even for loads as small as 5 nN.

Recently Buzio *et al.* reported a friction characterization on cluster-assembled carbon films produced by our technique³¹. They have found a non-linear dependence of friction on load, well fitted by the Hertzian-plus-offset model³², using a silicon tip of ~ 30 nm and scan length of 50 nm. On the other hand, a linear dependence of friction on load is found by scanning on a larger area ($1 \times 1 \mu\text{m}^2$)³³. The authors attributed the non-linear dependence to a possible passivation of the sample surface and to the presence of a water layer, which would induce a transition from a multi-asperity to a single-asperity contact (i.e. from a linear to a power-law dependence) as explained in the framework of the composite-tip model³⁴. For larger scan length and relatively larger scan velocity, the tip-sample interface is broken and re-formed rapidly and the smoothing action of water and impurities is less effective. This hypothesis is confirmed by our measurements apart from differences observed in the numerical values of the friction coefficients.

5. CONCLUSIONS

We have characterized by FFM-AFM the tribological properties of nanostructured carbon films grown by supersonic cluster beam deposition. We have found that the friction behavior at the nanoscale can be described by a modified Amonton's law demonstrating that a nanometer-sized contact not necessarily leads to a single-asperity friction regime. Molecular Dynamics simulations support our interpretation and show a qualitative agreement with the experiments. Our results show that the presence of water and the high reactivity of *sp*²-*sp*³ material plays an important role in determining a multi-asperity like contact also at these very small scales. Although numerical comparison with other carbon-based systems must be considered with high caution, cluster-assembled carbon shows a low friction coefficient even in a dry environment. The nanoscale structure of the films seem to have a negligible influence on the friction at the observed scales. This suggests that the tribological behavior of a nanostructured solid is "scale-sensitive" and one should always consider the scale factor before making comparison or extrapolations.

Acknowledgments

Partial financial support from Italian Space Agency is acknowledged.

References

- * Electronic address: `pmilani@mi.infn.it`; URL: `http://webcesid1.fisica.unimi.it/~labmilani/`
- ¹ B. Bhushan, *Handbook of Micro and Nano Tribology* (Chemical Rubber, Boca Raton, FL, 1995).
- ² R. Carpick and M. Salmeron, Chem. Rev. **97**, 1163 (1997).
- ³ MRS Bull. **26** (2001).
- ⁴ J. Sullivan, T. Freidmann, and K. Hjort, MRS Bull. **26**, 309 (2001).
- ⁵ S. Sundararajan and B. Bhushan, Wear **225/229**, 678 (1999).
- ⁶ P. Milani, P. Piseri, E. Barborini, A. Podestà, and C. Lenardi, J. Vac. Sci. Technol. **A19**, 2025 (2001).
- ⁷ D. Donadio, L. Colombo, P. Milani, and G. Benedek, Physical Review Letters **83**, 776 (1999).
- ⁸ E. Barborini, P. Piseri, A. Li Bassi, A. Ferrari, C. Bottani, and P. Milani, Chemical Physics Letters **300**, 633 (1999).
- ⁹ C. Casari, A. Li Bassi, C. Bottani, E. Barborini, P. Piseri, A. Podestà, and P. Milani, Phys. Rev. B **64**, 085417/1 (2001).
- ¹⁰ G. Dedkov, Phys. Stat. Sol. (a) **179**, 3 (2000).
- ¹¹ G. Adams and M. Nosonovsky, J. Trib. **33**, 431 (2000).
- ¹² V. Koinkar and B. Bhushan, J. Appl. Phys. **81**, 2472 (1997).
- ¹³ S. Sundararajan and B. Bushan, J. Appl. Phys. **88**, 4825 (2000).
- ¹⁴ F. Bowden and D. Tabor, *The Friction and Lubrication of Solids* (Clarendon, Oxford, 1950).
- ¹⁵ P. Milani and S. Iannotta, *Cluster Beam Synthesis of Nanostructured Materials* (Springer-Verlag, Berlin, 1999).
- ¹⁶ E. Barborini, P. Piseri, and P. Milani, Journal of Physics D (Applied Physics) **32**, L105 (1999).
- ¹⁷ P. Piseri, A. Podestà, E. Barborini, and P. Milani, Rev. Sci. Instrum. **72**, 2261 (2001).
- ¹⁸ J. Tersoff, Phys. Rev. B **37**, 6991 (1988).
- ¹⁹ J. Tersoff, Phys. Rev. Lett. **61**, 2879 (1988).
- ²⁰ W. Cheong and L. Zhang, Nanotechnology **11**, 173 (2000).
- ²¹ C. Mate, G. McClelland, R. Erlandsson, and S. Chiang, Phys. Rev. Lett. **59**, 1942 (1987).

- ²² K. Johnson, K. Kendall, and A. Roberts, Proc. R. Soc. Lond. **A324**, 301 (1971).
- ²³ A. Podestà, Ph.D. thesis, Università degli Studi di Milano (2002), unpublished.
- ²⁴ A. Podestà, G. Fantoni, P. Milani, C. Guida, and S. Volponi (2002), Thin Solid Film, in press.
- ²⁵ V. Koinkar and B. Bhushan, J. Vac. Sci. Technol. **A14**, 2378 (1996).
- ²⁶ C. Gibson, G. Watson, and S. Myhra, Nanotechnology **7**, 259 (1996).
- ²⁷ A. Grill, Surf. Coat. Technol. **94/95**, 507 (1997).
- ²⁸ M. Binggeli and C. Mate, Appl. Phys. Lett. **65**, 415 (1994).
- ²⁹ B. Bhushan and C. Dandavate, J. Appl. Phys. **87**, 1201 (2000).
- ³⁰ L. Ostrovskaya, V. Ralchenko, A. Podestà, and P. Milani, *Wettability and surface energy of cluster-assembled carbon films* (2002), to be published.
- ³¹ C. B. R. Buzio, E. Gnecco and U. Valbusa, Carbon **40**, 883 (2002).
- ³² U. Schwarz, O. Zworner, P. Koster, and R. Wiesendanger, Phys. Rev. B **56**, 6987 (1997).
- ³³ E. Gnecco, R. Buzio, C. Boragno, and U. Valbusa, Acta Phys. Slovaca **50**, 423 (2000).
- ³⁴ C. Putman and M. Igarashi, Appl. Phys. Lett. **66** (1995).
- ³⁵ One should keep in mind that we have measured the friction coefficient and adhesive offset of the pair (ns-carbon, Silicon AFM tip). Using AFM tips with different composition can lead in principle to different friction coefficients and adhesive offsets.
- ³⁶ The statistical error in each measurement is in general very small, because with our procedure we may acquire up to 512x512 friction-load pairs in each image and many images fast and reliably.

Figure captions

- Fig. 1. Representation of the model used for AFM-FFM molecular dynamics simulations. Only a ~ 50 Å thick top layer of nanostructured carbon film is shown. Color map reflects the coordination of atoms in the ns-carbon film: Blue, 1-fold coordinated; yellow, 2; green, 3; red, 4.
- Fig. 2. AFM pictures of a 250 nm thick ns-carbon film at different magnifications. The scan size is $2\text{ }\mu\text{m}$ (top) and 500 nm (bottom). The vertical color scale is 100 nm. The higher magnification picture clearly shows the surface granularity of such nanostructured films.
- Fig. 3 Lateral force vs. (external) applied load curve measured on ns-carbon.
- Fig. 4 Measured friction coefficients μ and friction offset c for films grown with large clusters and grown with small clusters in humid nitrogen (RH \sim 40%).
- Fig. 5 Measured friction coefficients μ and friction offset c for films grown with large clusters and grown with small clusters in dry nitrogen (RH \sim 2%).
- Fig. 6 Lateral force vs. applied load values and fitting from MD simulations, for sample (A) (circles and solid line) and for sample (B) (squares and dashed line). Error bars represent the standard deviation of the lateral force calculated for each scansion at a given load.

Figures

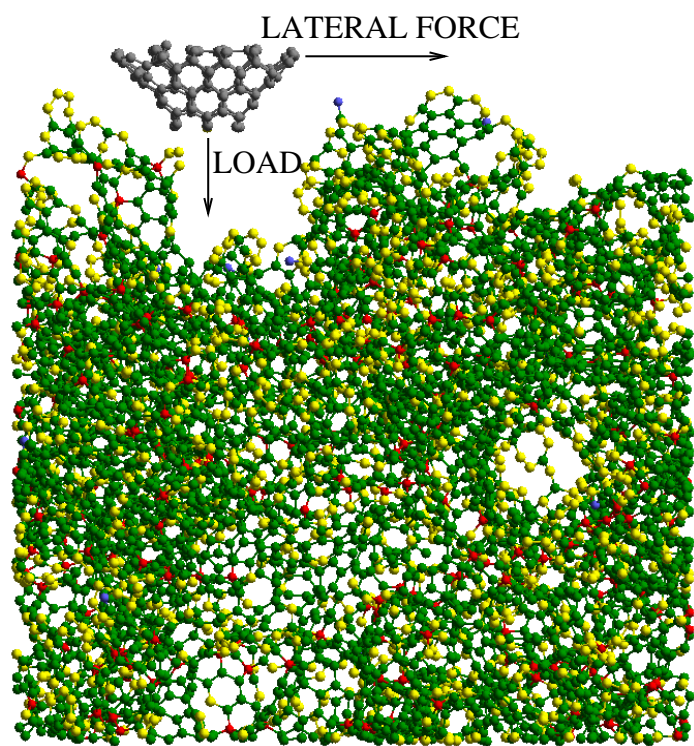


FIG. 1:

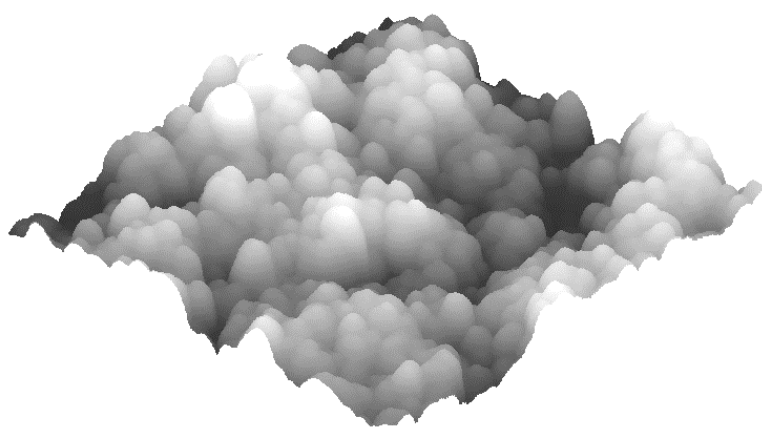
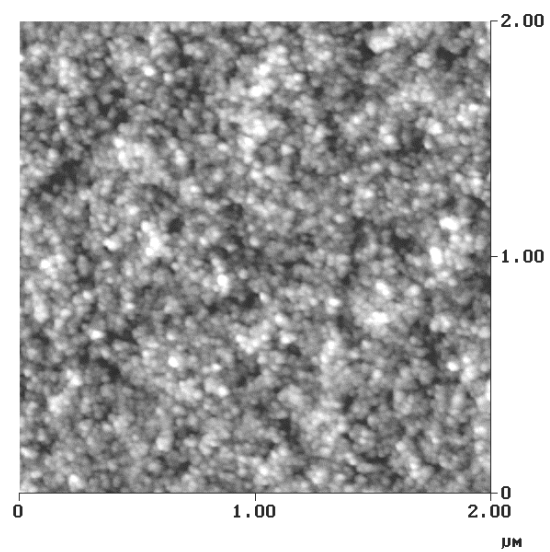


FIG. 2:

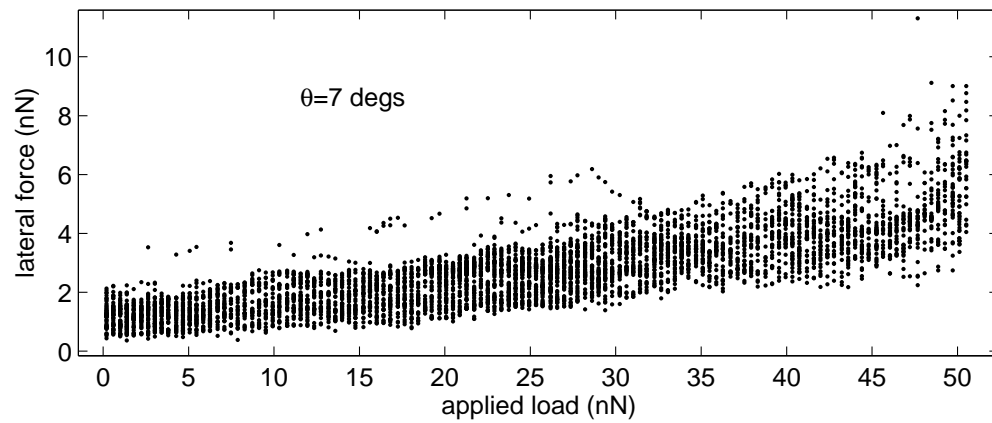


FIG. 3:

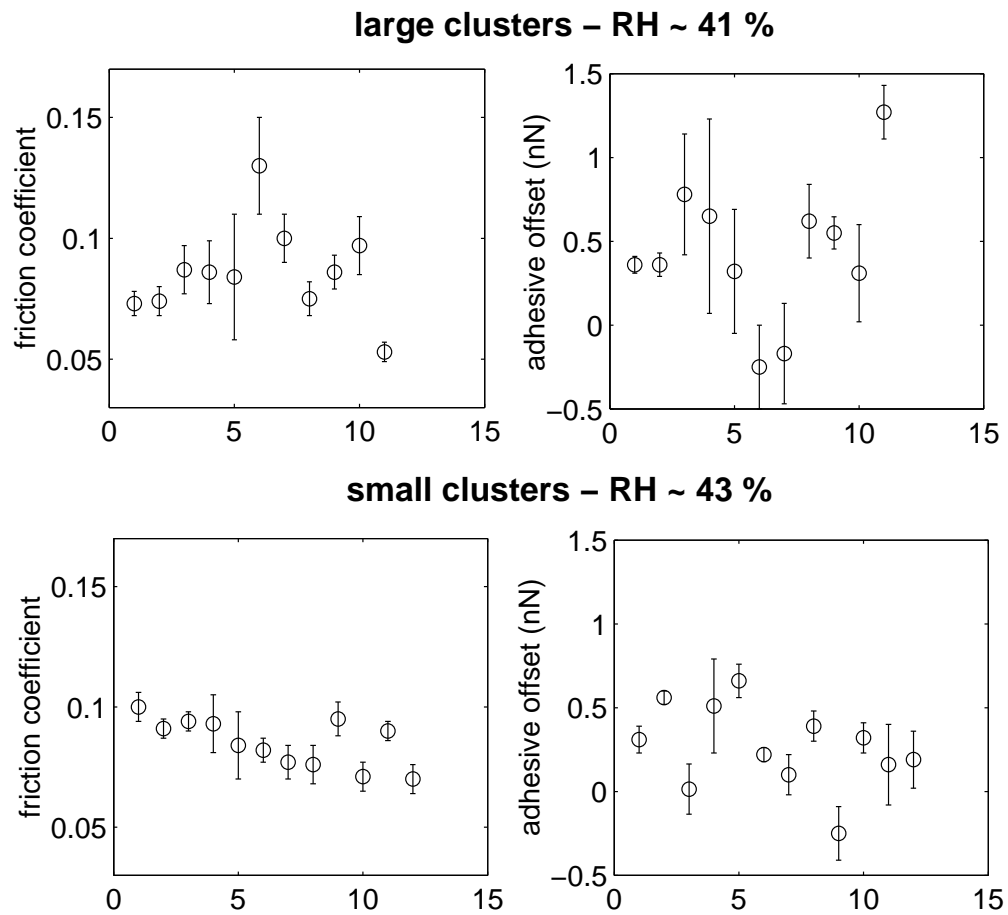


FIG. 4:

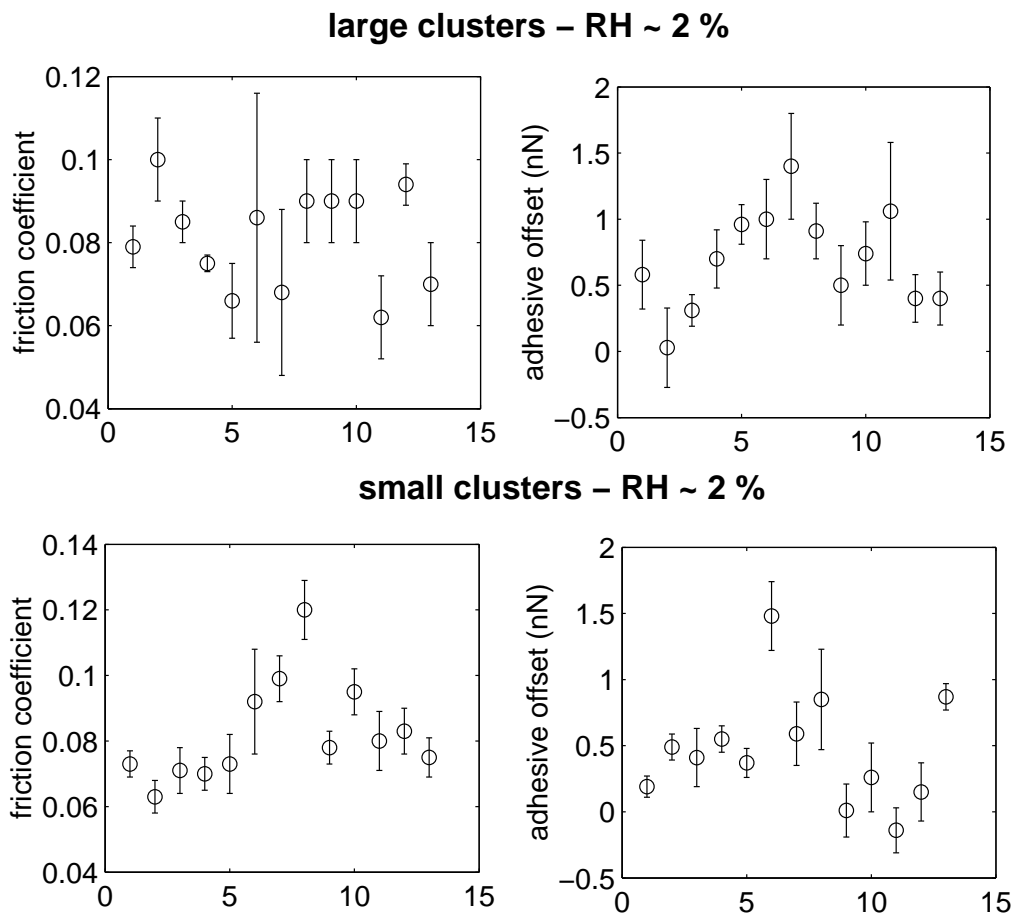


FIG. 5:

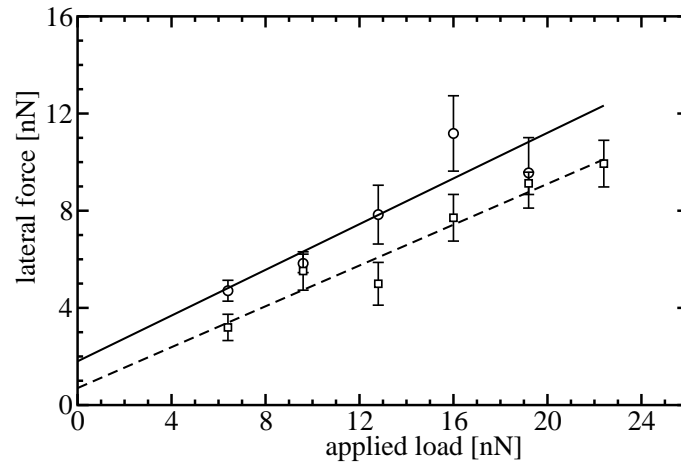


FIG. 6: